Myasthenic syndrome caused by mutation of the *SCN4A* sodium channel

Akira Tsujino*†, Chantal Maertens†‡, Kinji Ohno*, Xin-Ming Shen*, Taku Fukuda*, C. Michael Harper*, Stephen C. Cannon§¶, and Andrew G. Engel*

*Department of Neurology and Neuromuscular Research Laboratory and Department of Biochemistry and Molecular Biology, Mayo Clinic, Rochester, MN 55905; ‡Department of Neurology, Harvard Medical School, Boston, MA 02114; and §Department of Neurology, University of Texas Southwestern Medical Center, Dallas, TX 75390

Edited by Clay M. Armstrong, University of Pennsylvania School of Medicine, Philadelphia, PA, and approved April 23, 2003 (received for review January 16, 2003)

In a myasthenic syndrome associated with fatigable generalized weakness and recurrent attacks of respiratory and bulbar paralysis since birth, nerve stimulation at physiologic rates rapidly decremented the compound muscle action potential. Intercostal muscle studies revealed no abnormality of the resting membrane potential, evoked quantal release, synaptic potentials, acetylcholine receptor channel kinetics, or endplate ultrastructure, but endplate potentials depolarizing the resting potential to −40 mV failed to excite action potentials. Pursuing this clue, we sequenced *SCN4A* encoding the skeletal muscle sodium channel ($Na_v1.4$) and detected two heteroallelic mutations involving conserved residues not present in 400 normal alleles: S246L in the S4/S5 cytoplasmic linker in domain I, and V1442E in the S3/S4 extracellular linker in domain IV. The genetically engineered V1442E-Na channel expressed in HEK cells shows marked enhancement of fast inactivation close to the resting potential, and enhanced use-dependent inactivation on high-frequency stimulation; S246L is likely a benign polymorphism. The V1442E mutation in *SCN4A* defines a novel disease mechanism and a novel phenotype with myasthenic features.

In normal neuromuscular transmission, activation of acetylcholine receptors (AChRs) gives rise to an endplate potential (EPP) that activates voltage-dependent sodium channels ($Na_v1.4$). A high concentration of AChRs on crests of the synaptic folds (1) and of $Na_v1.4$ in the depth of the folds (2, 3) ensures that excitation is propagated beyond the endplate (EP) (4, 5). The safety margin of neuromuscular transmission is a function of the difference between the depolarization caused by the EPP and the depolarization required to activate $Na_v1.4$. All congenital or acquired defects of neuromuscular transmission identified to date have been traced to one or more factors that render the EPP subthreshold for activating $Na_v1.4$ (6, 7). We here describe a novel congenital myasthenic syndrome in which EPPs of normal amplitude fail to activate $Na_v1.4$, and trace the cause of the disorder to a mutation in *SCN4A* that markedly enhances fast-inactivation of $Na_v1.4$.

Materials and Methods

EP Studies. Intercostal muscle specimens were obtained from the patient and control subjects without muscle disease undergoing thoracic surgery. All human studies were in accord with the guidelines of the Institutional Review Board of the Mayo Clinic.

Measurement of number of AChRs per EP with ^{125}I-labeled α-bungarotoxin and localization of AChR and acetylcholinesterase at the EP were by described methods (8). Peroxidase-labeled α-bungarotoxin was used for the electron microscopy (EM) localization of AChR (9). The α subunit of Na_v1 sodium channels was immunolocalized in muscle with a polyclonal pan-sodium channel antibody (Alamone Labs, Jerusalem). EPs were localized for EM by established methods (10). Miniature EPP (MEPP) and EPP recordings and estimates of the number of transmitter quanta released by nerve impulse were carried out as described (8). Patch-clamp recordings from the EP AChRs were performed as described (11).

Sequencing Procedures. PCR-amplified fragments of *SCN4A* were cleared of unincorporated dNTPs and primers by using shrimp alkaline phosphatase (Amersham Biosciences/United States Biochemical) and exonuclease I (Amersham Biosciences/United States Biochemical) and incubated at 37°C for 15 min. The enzymes were then inactivated at 80°C for 15 min (12). Plasmids were purified by the QIAprep Spin Miniprep kit (Qiagen). PCR products and plasmids were sequenced with an ABI377 DNA sequencer (Applied Biosystems) using fluorescently labeled dideoxy terminators.

Mutation Analysis. DNA was isolated from muscle and blood as described (13). To sequence all 24 exons with their flanking noncoding regions of *SCN4A*, we synthesized 21 pairs of PCR primers based on the genomic sequence of *SCN4A* (GenBank accession no. AC005803) and directly sequenced the PCR products. We used allele-specific PCR to screen 400 normal alleles for the identified mutations. *CHAT*, the gene encoding choline acetyltransferase, was sequenced as described (14).

Because DNA from the patient's father was not available for genetic analysis, we examined the allelic distribution of S246L and V1442E by cloning a cDNA fragment and by haplotype analysis. For cDNA cloning, we used the long-distance reverse transcription method (15) to amplify a 4-kb cDNA fragment. mRNA was isolated from the patient's muscle by using the MicroFastTrack mRNA isolation kit (Invitrogen). We synthesized first-strand cDNA by using oligo(dT) primer with Superscript II (Invitrogen) in the presence of 170 mM trehalose (Fluka) and 766 mM sorbitol (Fluka). We performed nested touchdown RT-PCR with KlenTaq LA (CLONTECH) to amplify a cDNA fragment spanning positions 536–4388, where position +1 represents the translational start site. We then cloned the RT-PCR product by using the TOPO TA Cloning System (Invitrogen) and sequenced five clones that carried the expected insert.

For haplotype analysis, we analyzed four polymorphisms in intron 22 (IVS22 + 103C/A, IVS22 + 240T/C, IVS22 + 268C/T, and IVS22–242ins18) by direct sequencing. We also examined (CT)n dinucleotide repeat in intron 22 and (CT)n(CA)n dinucleotide repeats in intron 23 (16) by the GeneScan Analysis System (Applied Biosystems). To locate V1442E on the identified haplotypes, we PCR-amplified and

This paper was submitted directly (Track II) to the PNAS office.

Abbreviations: AChR, acetylcholine receptor; *CHAT*, gene encoding choline acetyltransferase; CMAP, compound muscle action potential; CMS, congenital myasthenic syndrome; EP, endplate; EPP, EP potential; MEPP, miniature EPP; *SCN4A*, gene encoding the adult muscle sodium channel, $Na_v1.4$.

Data deposition: The human *SCN4A* cDNA sequence reported in this paper has been deposited in the GenBank database (accession no. AY212253).

†A.T. and C.M. contributed equally to this work.

¶To whom correspondence should be addressed. E-mail: steve.cannon@utsouthwestern.edu.

PHYSIOLOGY

Table 1. Discordant nucleotides between our *SCN4A* clone and published sequences

Nucleotide*	Codon	Our clone	M81758†	L04216–L04236‡
28–30	10	GTG	GCT	—
		Val	Ala	—
31–33	11	CCT	CGT	—
		Pro	Arg	—
742–744	248	AAA	AAG	—
		Lys	Lys	—
1111–1113	371	GAG	AAG	CAG
		Glu	Lys	Gln
1675–1677	559	AAC	GAC	—
		Asn	Asp	—
2608–2610	870	GCG	—	GGC
		Ala	—	Gly
3451–3453	1151	AAC	—	AAG
		Asn	—	Lys
3454–3456	1152	GCC	—	CCC
		Ala	—	Pro
4126–4128	1376§	AAC	GAC	GAC
		Asn	Asp	Asp
5530–5532	—¶	CCC	CCCC	CCCC

Our clone has the same sequence as GenBank accession nos. L01962–L01983, NT_010783, and AC005803. Discordant nucleotides and codons are underlined. Em dashes indicate identity with our clone.
*Position +1 represent the first nucleotide of translational initiation codon.
†cDNA sequence reported by George *et al.* (19).
‡Genomic sequences reported by George *et al.* (21).
§N1376D is a known polymorphism (20).
¶Located in the 3′ noncoding region.

cloned a 2-kb genomic fragment spanning exons 22–24 from the patient's DNA, and sequenced 12 clones.

cDNA Cloning of Human *SCN4A*. We amplified the human *SCN4A* cDNA from the fetal skeletal muscle cDNA (Marathon-Ready cDNA, CLONTECH) by nested RT-PCR. We introduced the Kozak consensus sequence (5′-GCCGCCACC-3′) into the nested RT-PCR primer before the translational initiation site (17). The RT-PCR product was cloned into a pGEM-T vector (Promega), digested with *Eco*RI, excised from a gel, and then transferred to a cytomegalovirus (CMV)-based expression vector, pRBG4 (18). The insert corresponds to nucleotides 78–5631 of the published *SCN4A* cDNA sequence (19) (GenBank accession no. M81758), where the coding region is from nucleotide 78 to nucleotide 5588.

To confirm that there are no artifacts in our clone, we compared our sequence with the published *SCN4A* sequences. Our clone has the same coding sequence as GenBank accession nos. L01962–L01983 (20), NT_010783 (the National Center for Biotechnology Information Annotation Project), and AC005803 (the Human Genome Project), whereas M81758 (7) and L04216–L04236 (21) carry seven and six discordant nucleotides predicting five and five discordant amino acids, respectively (Table 1). Among these discordant amino acids, N1376D is a known polymorphism (20). We also sequenced four control human alleles and all alleles carried the same sequence as our clone. Therefore, our clone likely represents the consensus sequence of human *SCN4A*.

The S246L and V1442E missense mutations were introduced into pRBG4-*SCN4A* by using the QuikChange site-directed mutagenesis kit (Stratagene). Absence of unwanted artifacts was confirmed by sequencing the entire insert. Wild-type and mutant *SCN4A* clones were prepared for expression studies with the HiSpeed Plasmid Maxi Kit (Qiagen).

Whole-Cell Recording. Sodium currents were recorded from human embryonic kidney (HEK) cells transiently transfected with wild-type or mutant pRBG4-*SCN4A,* the accessory β_1 subunit (pGW-*SCN1B*), and a CD8 expression marker as described (22). The pipette (internal) solution contained 90 mM CsF, 35 mM NaC1, 10 mM EGTA, 10 mM Hepes, 1 mM $MgC1_2$, 5 mM Na_2ATP, and 5 mM Na_2-phosphocreatine (pH 7.4 by NaOH). The bath contained 140 mM NaC1, 4 mM KC1, 10 mM Hepes, 5 mM glucose, 1 mM $MgC1_2$, and 2 mM $CaC1_2$ (pH 7.4 by NaOH). Recordings were made at room temperature (21–23°C).

Results

Clinical Data. A 20-year-old normokalemic woman had abrupt attacks of respiratory and bulbar paralysis since birth lasting 3–30 min recurring one to three times per month. Since infancy, she has been on an apnea monitor and received ventilatory support during apneic attacks. She had delayed motor development, was always easily fatigued, and had droopy eyelids. At age 20, she had eyelid ptosis, limited ocular ductions, and facial, trunkal, and limb muscle weakness worsened by activity; she could walk less than half a block and could elevate her arms to the horizontal for only 20 sec. She had a high-arched palate, adduction deformity of the knees and ankles, and increased lumbar lordosis. She was mentally retarded; her brain MRI revealed mild cerebral atrophy that was attributed to previous episodes of cerebral anoxia. Tests for anti-AChR antibodies were negative. The patient's mother and sister were asymptomatic. No clinical data or DNA were available from the patient's father.

Nerve Stimulation Studies. Trains of stimuli at 2, 10, and 50 Hz were used to elicit compound muscle action potentials (CMAPs) from small hand muscles. In the patient, 10-Hz stimulation for 5 min, or 50-Hz stimulation for 2 sec, decremented the CMAP by ≈85%. A 2-Hz stimulation did not decrement the CMAP in rested muscle but elicited a 50% decrement after a conditioning train of 10-Hz stimuli for 1 min (Fig. 1 *A–D*). In a control, 10-Hz stimulation for 5 min reduced the CMAP only by ≈35%, 50-Hz stimulation for 2 sec caused pseudofacilitation (increased amplitude with proportionate decrease in area), and 2-Hz stimulation elicited no decrement before or after 10-Hz stimulation for 5 min (Fig. 1 *E–H*). Thus, sustained high-frequency stimulation, or low-frequency stimulation after a conditioning train of high-frequency stimulation, reduced the safety margin of neuromuscular transmission in the patient.

Muscle Histology. None of the intercostal muscle fibers harbored vacuoles of the type often observed in periodic paralysis muscle specimens. Type 1 fibers had a smaller mean diameter than type 2 fibers. The random distribution of the histochemical fiber types was maintained.

EP Studies. The number of AChR per EP, determined with ^{125}I-labeled α-bungarotoxin, was normal. The muscle fiber membrane potential was similar to that recorded from control muscle fibers (Table 2). EPPs of the order of 40 mV depolarizing the membrane potential to −40 mV or more failed to trigger action potentials and were recorded in the absence of D-tubocurarine (Fig. 2*A*). The MEPP amplitude and quantal content of the EPP were normal. Ten-hertz stimulation for 5 min decreased the EPP only by ≈13% (Fig. 2*B*) (normal <30%, ref. 23). Patch-clamp recordings from three EPs revealed AChR channels opening to a normal conductance of ≈60 pS and a channel opening burst of normal duration (Table 2).

Immunolocalization of sodium channels with an anti-pan sodium channel antibody showed similar surface membrane and similarly enhanced synaptic expression at patient and control muscle fibers (Fig. 3). EM examination of 63 regions of 34 EPs

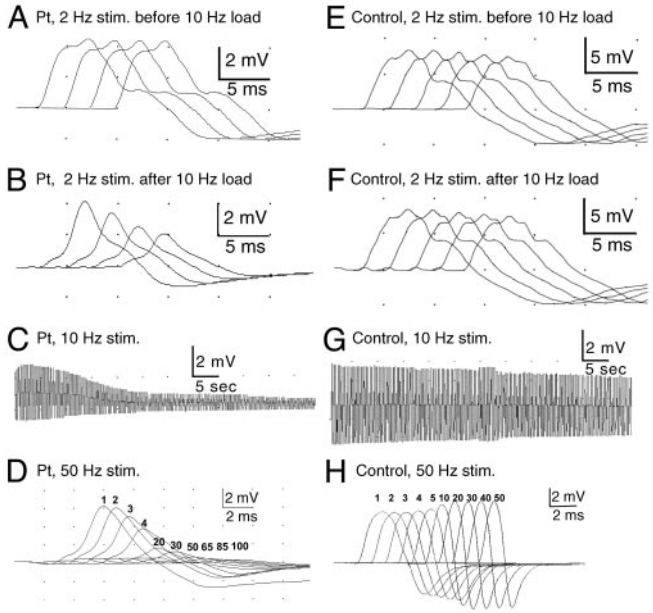

Fig. 1. Hypothenar CMAP in patient (*A–D*) and thenar CMAP in control (*E–H*) evoked by stimulation at 2, 10, and 50 Hz. Ten-hertz stimulation for 5 min (*C*) or 50-Hz stimulation for 2 sec (*D*) decrement the patient CMAP by ≈85%; 2-Hz stimulation for 2 sec has no effect on the patient CMAP unless it is preceded by a 10-Hz conditioning train (*A* and *B*). Control CMAP decrements slightly after 10-Hz stimulation (*G*), pseudofacilitates after 50-Hz stimulation (*H*), and is unaffected by 2-Hz stimulation before or after a 10-Hz conditioning train (*E* and *F*). Numbers in *D* and *H* indicate *n*th CMAPs elicited during 50-Hz stimulation.

revealed normal nerve terminals and well developed junctional folds at all EPs. A single postsynaptic region was denuded of its nerve terminal. The density and distribution of AChR on the crests of the junctional folds, determined with peroxidase-labeled α-bungarotoxin, was normal.

Table 2. Endplate studies

	Controls	Patient
[^{125}I]α-bgt binding sites/EP	12.82 ± 0.79 E6 (13)	11.51 E6
Resting membrane potential, mV*	−72.5 ± 0.78 (75)	−75.5 ± 1.4 (13 fibers)
EPP amplitude, mV†	ND	42.6 ± 5.05 (12)
Quantal release at 1 Hz‡	31 ± 1 (190)	36 ± 4.3 (12)
MEPP amplitude, mV§	1.00 ± 0.025 (165)	1.17 ± 0.08 (9)
Single-channel opening bursts¶		
τ_2, ms	0.12 ± 0.012 (32)	0.067 ± 0.0078 (3)
Area	0.16 ± 0.014	0.16 ± 0.025
τ_2, ms	3.04 ± 0.175 (34)	2.91 ± 0.32 (3)
Area	0.85 ± 0.015	0.84 ± 0.024

Values indicate mean ± SEM. Measurements were made at 30°C for MEPPs and EPPs and at 22°C for single-channel recordings. Numbers in parentheses indicate number of subjects for [^{125}I]α-bgt binding sites/EP and number of fibers or EPs for other measurements.

*Measured with 10–15 MΩ glass microelectrodes.

†Corrected for a resting membrane potential of −80 mV and nonlinear summation.

‡Corrected for a resting membrane potential of −80 mV, nonlinear summation, and non-Poisson release.

§Corrected for resting membrane potential of −80 mV and for a fiber diameter of 50 μm.

¶ACh, 1 μM; pipette potential, 80 mV; bandwidth, 5.8 kHz.

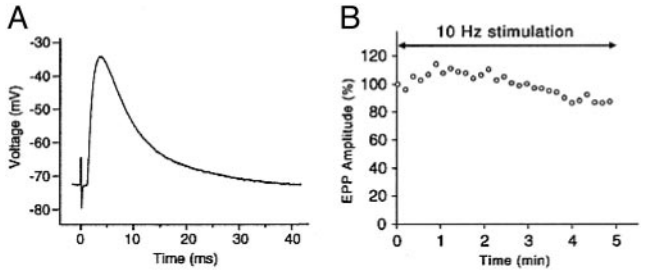

Fig. 2. (*A*) EPP recorded from patient intercostal muscle depolarizes the resting potential from −73 to −43 mV but fails to elicit an action potential. (*B*) The EPP elicited by 10-Hz nerve stimulation over 5 min first facilitates and then decreases by −13% from baseline. Individual symbols represent means of 100 EPPs recorded over 10-sec intervals.

To summarize, nerve stimulation studies combined with *in vitro* analysis of neuromuscular transmission indicate that physiologic rates of stimulation compromise the safety margin of neuromuscular transmission. The effect on the safety margin cannot be accounted for by a decreased amplitude of the EPP at rest or after protracted 10-Hz stimulation, by a deficiency or kinetic abnormality of AChR, by an alteration of the EP geometry, or by a paucity of junctional or extrajunctional sodium channels.

Mutation Analysis. Because some features of the patient's illness resembled the CMS caused by mutations in *CHAT* (14, 24), we first sequenced *CHAT* but observed no mutations. That EPPs depolarizing the muscle fiber membrane potential to −40 mV failed to activate action potentials prompted us to search for a mutation *SCN4A* that encodes $Na_v1.4$. We therefore directly sequenced the 24 exons with their flaking noncoding regions of *SCN4A* and identified two missense mutations. The first mutation is a C-to-T transition at nucleotide 737, where the position +1 represents the translational start site, predicting S246L in the cytoplasmic link between the S4 and S5 segments of domain I. The second mutation is a T-to-A transversion at nucleotide 4325, predicting V1442E in the extracellular link between the S3 and S4 segments of domain IV (Fig. 4). Neither S246L nor V1442E was observed in 400 normal alleles. Both S246 and V1442 are

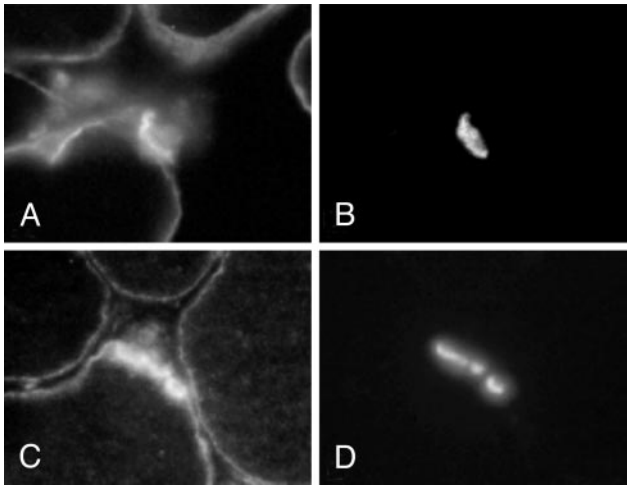

Fig. 3. Sodium channel (*A* and *C*) and AChE (*B* and *D*) localization in patient (*A* and *B*) and control (*C* and *D*) muscle fibers. EPs are identified by localization of AChE in the same sections. Sodium channel expression is similar at the surface membrane and is similarly enhanced at the EP in patient and control fibers. (Magnification, ×370.)

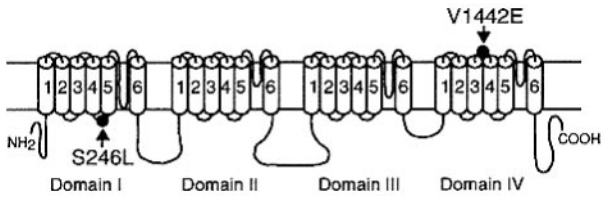

Fig. 4. Scheme of skeletal muscle sodium channel $Na_v1.4$ encoded by *SCN4A* and the identified mutations.

conserved across $Na_v1.4$ channels of different species. S246L is conserved across the α subunits of human sodium channels $Na_v1.1$ to $Na_v1.5$, $Na_v1.8$, and $Na_v1.9$; V1442 is similarly conserved except for the α subunit of $Na_v1.5$. The patient also carries a previously unreported G524D polymorphism, detected in 2 of 24 in controls.

Family analysis indicates that the asymptomatic mother and sister are heterozygous for S246L. Because the father's DNA was not available for genetic analysis, we examined the allelic distribution of S246L and V1442E by cloning a cDNA fragment and by haplotype analysis. Cloning of a 4-kb RT-PCR product spanning S246L and V1442E from the patient's muscle revealed that the mutations are heteroallelic. We also found a G524D polymorphism in the allele harboring V1442E. Haplotype analysis using three single-nucleotide polymorphisms, one insertion polymorphism, and two polymorphic dinucleotide repeats in introns 22 and 23 confirmed the heteroallelic distribution of the two mutations.

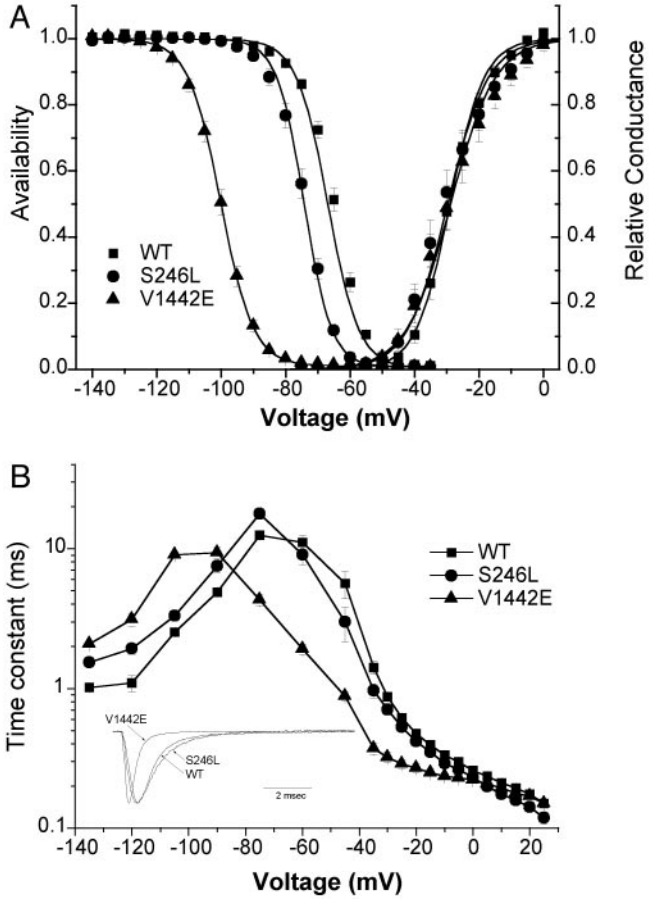

Fig. 5. Gating behavior of heterologously expressed sodium channels. (*A*) Channel availability (left) after a 300-msec prepulse was left-shifted for mutant channels, whereas activation (right) was unchanged. Parameter values for Boltzmann fits are listed in Table 3. (*B*) The kinetics of fast-inactivation were left-shifted for mutant channels (n = 7–12). Inactivation kinetics were measured as: recovery at −135 to −80 mV after 30-msec prepulse to −10 mV, closed-state entry with progressively longer prepulses over a range from −60 to −45 mV, or as the current decay rate for test depolarization ≥ −45 mV. For V1442E, the recovery/prepulse voltages for the inactivation protocols were shifted by −30 mV, to detect Na current in the presence of the large left-shift of inactivation. (*Inset*) Superposition of amplitude-normalized responses for a depolarization to −30 mV from a holding potential of −120 mV.

Table 3. $Na_v1.4$ gating behavior

Channel	Wild type	S246L	V1442E
Activation			
$V_{1/2}$, mV	−29.0 ± 1.2 (7)	−29.7 ± 2.0 (12)	−28.8 ± 2.2 (8)
k, mV	5.3 ± 0.3 (7)	6.3 ± 0.5 (12)	6.9 ± 0.3 (8)
Fast-inactivation			
$V_{1/2}$, mV	−66.9 ± 1.2 (11)	−74.2 ± 0.8 (17)	−100.1 ± 0.8 (11)
k, mV	4.8 ± 0.1 (11)	4.2 ± 0.1 (17)	5.0 ± 0.1 (11)
Slow-inactivation			
$V_{1/2}$, MV	−52.9 ± 2.4 (5)	−72.5 ± 3.0 (8)	−49.9 ± 1.8 (4)
k, mV	12.3 ± 1.0 (5)	10.8 ± 0.5 (8)	14.5 ± 0.5 (4)
Io	0.17 ± 0.03 (5)	0.32 ± 0.04 (8)	0.11 ± 0.02 (4)

Voltage dependence of relative current was fit by a Boltzmann function except for slow-inactivation, which was fit with a Boltzmann plus a constant: $I = Io + (1 - Io)/(1 + \exp((V - V_{1/2})/k))$. Numbers in parentheses indicate number of cells.

Heterologous Expression Studies. Our wild-type construct and both mutants expressed at levels comparable to the previously published cDNA for $Na_v1.4$ (19) as judged by current density. Channel activation by depolarization was not altered by either mutation (Fig. 5*A*, right). The voltage dependence of fast inactivation produced by a 300-msec conditioning pulse was markedly left-shifted by −33 mV for the V1442E mutant, whereas the S246L mutant had a milder shift of −7 mV (Fig. 5*A* and Table 3). This shift in steady-state behavior was accompanied by a commensurate left shift in the voltage-dependence for the kinetics of fast inactivation (Fig. 5*B*). The limiting value for the time constant of current decay at positive test potentials reflects the microscopic inactivation rate from the open state (25) and was not affected by either mutation. Neither mutation disrupted the completeness of fast inactivation, as revealed by the lack of an increased persistent Na current at the end of a 10-msec depolarization (Fig. 5*B Inset*).

Sodium channel mutations found in periodic paralysis often disrupt slow inactivation (26). We assessed slow inactivation by applying a 30-sec conditioning pulse, followed by recovery at −120 mV for 20 msec to remove fast inactivation and a test depolarization to −10 mV. The V1442E mutation did not affect slow inactivation, whereas a mixed effect was observed for S247L: enhancement of slow inactivation by a −20 mV leftward shift, and impaired maximal extent of slow inactivation at depolarized potentials (Fig. 6 and Table 3).

The response to a 50-Hz train of 3-msec pulses was measured to assess whether use-dependent Na channel inactivation might contribute to the abnormal decremental CMAP response observed in the patient's muscle at high-frequency stimulation. The normalized peak current amplitude had a precipitous drop of 30% during the first few pulses for the V1442E mutant, whereas wild-type and S246L channels showed only a 5% decrease (Fig. 7). The rapid decrement is caused by trapping of V1442E channels in the fast-inactivated state because recovery at −100 mV is slowed 3-fold for this mutant (Fig. 5*B*). Conversely, the lack of a difference between wild-type and S246L channels after 200 pulses suggests that neither the alterations in slow inactiva-

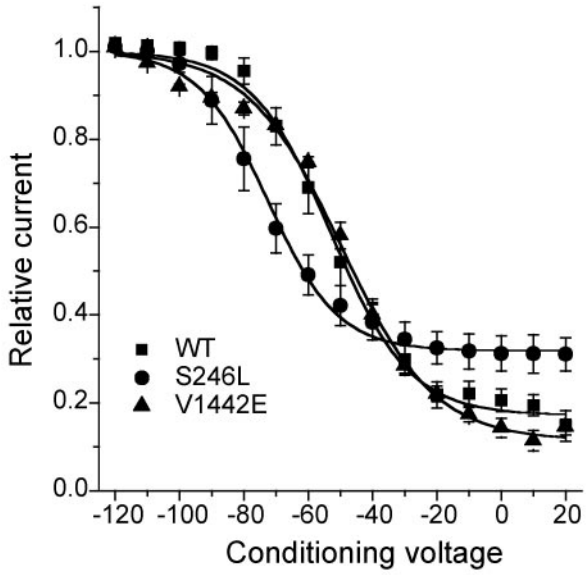

Fig. 6. Slow inactivation after a 30-sec conditioning pulse, and an intervening recovery at −120 mV for 20 msec to remove fast inactivation, was less complete for S246L and shifted toward more negative potentials (see Table 3 for fitted parameters).

tion nor the milder shift in fast inactivation for S246L is sufficient to produce abnormal use dependence during 50-Hz stimulation.

Discussion

The Clinical Features Herald a Myasthenic Phenotype. The patient's fatigable weakness involving lid-elevator, external ocular, and facial as well as limb and trunkal muscles and the decremental response of the CMAP on repetitive stimulation were consistent with a myasthenic phenotype. The patient's apneic attacks and the requirement for a conditioning train of stimuli at 10 Hz to elicit a decremental response at 2-Hz stimulation closely mimic features of a presynaptic CMS caused by mutations in *CHAT* (14, 24). In the present disorder, however, the stimulation-dependent decrement of the CMAP is not owing to impaired resynthesis of acetylcholine and concomitant abnormal decrease of the EPP, but stems from a defect in $Na_v1.4$. Other factors that compromise neuromuscular transmission in previously recognized congenital myasthenic syndromes, e.g., decrease of evoked quantal release, diminished expression of AChE or AChR, a kinetic defect in AChR, or alteration of EP geometry, were excluded by the EP studies.

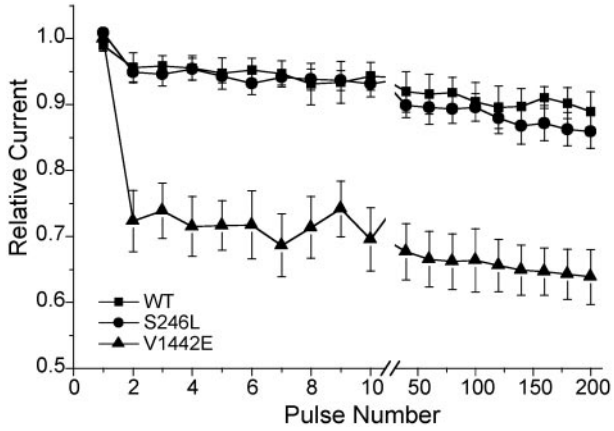

Fig. 7. Relative Na current during a 50-Hz train of 3-msec depolarizations to −10 mV from a holding potential of −100 mV. Every 20th response is shown after the break at the 10th pulse.

The present phenotype differs from that of periodic paralyses associated with hitherto identified mutations of *SCN4A*. The onset is neonatal, the disorder is normokalemic, the attacks selectively involve bulbar and respiratory muscles, physiologic rates of stimulation decrement the CMAP abnormally, and the muscle fiber membrane potential is normal when action potential generation fails. Periodic paralyses stemming from mutations in *SCN4A* present later in life, the attacks typically spare cranial, bulbar, and respiratory muscles, the serum potassium level increases or declines during attacks in most cases, mild exercise for brief periods does not decrement the CMAP, and the resting membrane potential of the muscle fiber is decreased when action potential generation fails (27, 28).

Relation to Other Na Channel Diseases. Mutations in the coding region of voltage-gated sodium channels are known to be a cause of epilepsy and cardiac arrhythmia, in addition to skeletal muscle disorders with myotonia, periodic paralysis, and now congenital myasthenia features (28). All of these disorders are inherited as dominant traits, and the mutant channels are functional, albeit with altered gating behavior. Most of these mutations produce gain-of-function defects wherein impairment of inactivation, or less commonly enhanced activation, results in excessive inward Na current. At the cellular level, the aberrant current may induce autonomous firing (myotonia), delayed repolarization (cardiac long QT), or prolonged depolarization and block of action potentials (periodic paralysis). Each of these defects occurs because of the tendency for the excessive activity mutant channels to depolarize the cell. In contrast, loss-of-function defects consistently occur in only a subset of periodic paralysis: those with features of hypokalemic periodic paralysis (HypoPP) due to mutations in $Na_v1.4$ (28, 29). As expected for a loss-of-function, action potentials in affected muscle have smaller overshoots and slower rates of rise. The defect described herein is a more extreme example, with complete failure of action potential initiation by a normal EPP (Fig. 2). Commensurate with this more pronounced defect in excitability, the leftward (hyperpolarized) shift for inactivation was much greater for V1442E (−30 mV, Fig. 5*A*) than the −10 mV shift observed for R672 mutants in HypoPP.

Mechanisms Accounting for Reduced Availability of Functional $Na_V1.4$. The loss-of-function defect in this case of congenital myasthenic syndrome is attributable to the left shift in the voltage dependence of fast inactivation. Depolarization induces outward movement of all four S4 voltage sensors, but fast inactivation is only linked to S4 movements of domains III and IV (30). The enhanced inactivation of V1442E can be explained by a mutation-induced bias in the voltage-dependent motion of IV/S4 toward the outward conformation. In contrast, mutations at the arginine residues of IV/S4 that cause myotonia and slow the rate of inactivation (31) are presumably because of an effect on the rate of a conformational change rather than on inducing bias.

At the normal resting potential of −90 mV, 98% of wild-type channels remain available, whereas for V1442E channels the availability is only 13% (Fig. 5*A*). The defect is compounded by enhanced cumulative use-dependent inactivation (Fig. 7), which further reduces V1442E channel availability and may explain the abnormal CMAP decrement observed at high-frequency stimulation (Fig. 1). The bias of having the majority of wild-type channels non-inactivated at −90 mV may have evolved to ensure rapid recovery and thereby minimize use dependence at physiological rates of discharge. S246L also shifts the availability curve to the left (Fig. 5*A*), but this −7 mV shift alone is clinically silent (unaffected mother and sister), compared with the −10

mV shift purported to cause HypoPP for the R672G/H mutations (28).

The inheritance pattern for this case of congenital myasthenic syndrome cannot be unambiguously established. The more severe V1442E mutation may be dominant, but this cannot be proven because this mutation was observed only in combination with the heteroallelic S246L mutation. The S246L mutation alone was clinically silent and therefore either represents a rare polymorphism with detectable biophysical changes, but no clinical or EMG phenotype, or a recessive mutation. Despite this uncertainty, this report clearly establishes a congenital myasthenic syndrome as a new allelic disorder to be grouped with the myotonias and periodic paralyses previously attributed to mutations in $Na_v1.4$. Our findings also have therapeutic implications: After the defect in $Na_v1.4$ was established in the patient, therapy with pyridostigmine (60–120 mg three times daily), which increases the number of AChRs activated by each quantum, improved the patient's endurance; additional therapy with acetazolamide (250 mg twice daily), which is known to mitigate periodic paralysis due to $Na_v1.4$ mutations, prevented further attacks of respiratory and bulbar weakness. Moreover, this study demonstrates that a reduced margin of safety for neuromuscular transmission may occur in the setting of a normal EPP.

We thank Dr. M. Takagishi and Dr. G. A. Ristow for patient referral. This work was supported by National Institutes of Health Grants NS6277 (to A.G.E.) and AR42703 (to S.C.C.), and a Muscular Dystrophy Association grant (to A.G.E.). C.M. is an Aspirant of the Fonds voor Wetenschappelijk Onderzoek–Vlaanderen.

1. Salpeter, M. M. (1987) in *Vertebrate Neuromuscular Junctions: General Morphology, Molecular Organization, and Functional Consequences*, ed. Salpeter, M. M. (Liss, New York), pp. 1–54.
2. Flucher, B. E. & Daniels, M. P. (1989) *Neuron* **3,** 163–175.
3. Ruff, R. L. (1996) *Acta Physiol. Scand.* **156,** 159–168.
4. Martin, A. R. (1994) *Proc. R. Soc. London B* **258,** 321–326.
5. Wood, S. J. & Slater, C. P. (2001) *Prog. Neurobiol.* **64,** 393–429.
6. Harper, C. M. (1999) in *Electrodiagnosis of Endplate Disease*, ed. Engel, A. G. (Oxford Univ. Press, New York), pp. 65–84.
7. Engel, A. G., Ohno, K. & Sine, S. M. (2002) *Mol. Neurobiol.* **26,** 347–367.
8. Engel, A. G., Nagel, A., Walls, T. J., Harper, C. M. & Waisburg, H. A. (1993) *Muscle Nerve* **16,** 1284–1292.
9. Engel, A. G., Lindstrom, J. M., Lambert, E. H. & Lennon, V. A. (1977) *Neurology* **27,** 307–315.
10. Engel, A. G. (1994) in *Myology*, eds. Engel, A. G. & Franzini-Armstrong, C. (McGraw–Hill, New York), 2nd Ed., pp. 1018–1045.
11. Milone, M., Hutchinson, D. O. & Engel, A. G. (1994) *Muscle Nerve* **17,** 1364–1369.
12. Dorit, R. L., Ohara, O., Wang, C. B. C., Kim, J. B. & Blackshaw, S. (2001) in *Current Protocols in Molecular Biology*, eds. Ausubel, F. M., Brent, R., Kingston, R. E., Moore, D. D., Seiman, J. G., Smith, J. A. & Struhl, K. (Wiley, New York), pp. 15.2.
13. Ohno, K., Hutchinson, D. O., Milone, M., Brengman, J. M., Bouzat, C., Sine, S. M. & Engel, A. G. (1995) *Proc. Natl. Acad. Sci. USA* **92,** 758–762.
14. Ohno, K., Tsujino, A., Brengman, J. M., Harper, C. M., Bajzer, Z., Udd, B., Beyring, R., Robb, S., Kirkham, F. J. & Engel, A. G. (2001) *Proc. Natl. Acad. Sci. USA* **98,** 2017–2022.
15. Carninci, P., Shiraki, T., Mizuno, Y., Muramatsu, M. & Hayashizaki, Y. (2002) *BioTechniques* **32,** 984–985.
16. McClatchey, A. I., Trofatter, J., McKanna-Yasek, D., Easkind, W., Bird, T., Pericak-Vance, M., Gilchrist, J., Arahata, K., Radosavljevic, D. & Worthen, H. G. (1992) *Am. J. Hum. Genet.* **50,** 896–901.
17. Kozak, M. (1987) *Nucleic Acids Res.* **15,** 8125–8148.
18. Ohno, K., Wang, H.-L., Milone, M., Bren, N., Brengman, J. M., Nakano, S., Quiram, P., Pruitt, J. N., Sine, S. M. & Engel, A. G. (1996) *Neuron* **17,** 157–170.
19. George, A. L., Jr., Komisarof, J., Kallen, R. G. & Barchi, R. L. (1992) *Ann. Neurol.* **31,** 131–137.
20. McLatchey, A. I., Lin, C. S., Wang, J., Hoffman, E. P., Rojas, C. & Gusella, J. F. (1992) *Hum. Mol. Genet.* **1,** 521–527.
21. George, A. L., Jr., Iyer, G. S., Kleinfeld, R., Kallen, R. G. & Barchi, R. L. (1993) *Genomics* **15,** 598–606.
22. Hayward, L. J., Brown, R. H. & Cannon, S. C. (1996) *J. Gen. Physiol.* **107,** 559–576.
23. Engel, A. G. & Lambert, E. H. (1987) *Electroencephalogr. Clin. Neurophysiol. Suppl.* **39,** 91–102.
24. Mora, M., Lambert, E. H. & Engel, A. G. (1987) *Neurology* **37,** 206–214.
25. Aldrich, R. W., Corey, D. P. & Stevens, C. F. (1983) *Nature* **306,** 436–441.
26. Cannon, S. C. (2002) *Neuromuscul. Disord.* **12,** 533–543.
27. Engel, A. G., Potter, C. S. & Rosevear, J. W. (1965) *Am. J. Med.* **38,** 626–640.
28. Lehmann-Horn, F. & Jurkat-Rott, K. (1999) *Physiol. Rev.* **79,** 1317–1372.
29. Struyk, A. F., Scoggan, K. A., Bulman, D. E. & Cannon, S. C. (2000) *J. Neurosci.* **20,** 8610–8617.
30. Cha, A., Ruben, P. C., George, A. L., Jr., Fujimoto, E. & Bezanilla, F. (1999) *Neuron* **22,** 73–87.
31. Yang, N., Ji, S., Zhou, M., Ptacek, L. J., Barchi, R. L., Horn, R. & George, A. L., Jr. (1994) *Proc. Natl. Acad. Sci. USA* **91,** 12785–12789.